端面抽运 Nd:YAG/Cr^{4+}:YAG/KTA 被动调 Q 级联拉曼激光器

齐子钦[1], 毛文杰[1], 王鸿雁[2], 朱小龙[1], 裘馨楠[1], 陆欢洽[1], 朱海永[1*]

(1. 温州大学 电气与电子工程学院 温州市微纳光电器件重点实验室, 浙江 温州 325035;
2. 青岛海泰光电技术有限公司, 山东 青岛 266100)

摘 要: 报道了基于 KTA 晶体 671 cm^{-1} 和 234 cm^{-1} 频移的 LD 端面抽运被动调 Q 级联拉曼激光器。采用 Nd:YAG/Cr^{4+}:YAG 复合晶体产生被动调 Q 的脉冲基频激光来驱动 KTA 晶体,研究了不同入射抽运功率下级联拉曼激光的输出功率、光谱和脉冲特性。随着抽运功率的增加,输出激光波长从以 671 cm^{-1} 和 234 cm^{-1} 频移级联拉曼的 1178 nm 单波长过渡到与 1212 nm 同时输出的双波长。在 10.05 W 的入射抽运功率下,获得了 280 mW 平均输出功率,6.2% 转化效率的双波长激光。对应的脉冲宽度和重复频率分别为 1.2 ns 和 10.3 kHz,单脉冲能量和峰值功率分别为 27.2 μJ 和 22.7 kW。结果表明:基于 KTA 两个相当增益强度的频移,结合腔镜镀膜控制可以获得丰富的斯托克斯激光波长。

关键词: 拉曼激光; KTA 晶体; 被动调 Q; YAG 晶体

中图分类号: O436 **文献标志码:** A **DOI:** 10.3788/IRLA20230079

0 引 言

砷酸钛氧钾晶体 (KTA) 属于非线性光学晶体 KTP 的同构体,不仅具有较大的非线性系数和良好的物理化学和机械性能,而且拥有更宽的透光波段、更高的损伤阈值和导热性能[1−2]。因此,KTA 晶体在光参量振荡获得高效的人眼安全激光和中红外激光研究中被广泛应用[3−6]。1991 年, Watson[7] 首次报道了 KTA 晶体的拉曼光谱,并表明 234 cm^{-1} 频移具有较强的拉曼增益。近年来,KTA 晶体在受激拉曼激光器中优异的表现受到人们广泛的关注[8−10]。

受激拉曼散射 (SRS) 是一种高强度的三阶非线性光学现象,具有波长转换灵活、无需相位匹配等优势。至今,金刚石、钒酸盐、钨酸盐等许多晶体被证明具有较强的拉曼增益[11−14],被广泛应用于高效的拉曼激光器设计。而 KTA 晶体同时是二阶非线性光学晶体,相对以上常见拉曼晶体可同时实现受激拉曼散射和二阶非线性变频 [15−17],而且其增益较大的拉曼频移量较小,更有利于通过级联拉曼输出高阶斯托克斯激光。2008 年,山东大学 Liu 等[18] 报道了基于 KTA 晶体 234 cm^{-1} 拉曼频移的 1120 nm 二阶斯托克斯激光。2013 年, Lan 等[19] 采用端面抽运 Nd:YAG/KTA 被动调 Q 获得了 250 mW 输出功率、3.3% 转换效率的 1091 nm 一阶斯托克斯激光。2016 年,笔者课题组[20] 利用声光调 Q 基频偏振特性结合 KTA 晶体不同拉曼构型增益的差异,通过旋转 KTA 晶体分别实现了 1.15 μm 波段的 234 cm^{-1} 拉曼频移的三阶斯托克斯激光和 671 cm^{-1} 拉曼频移的一阶斯托克斯激光。结果表明 KTA 晶体 234 cm^{-1} 和 671 cm^{-1} 拉曼频移都可以实现高效的拉曼频移激光。最近,团队基于 Nd:YAG/Cr^{4+}:YAG/KTA 被动调 Q 拉曼自倍频,成功实现了 671 cm^{-1} 拉曼频移的一阶斯托克斯倍频输出[21]。

Cr^{4+}:YAG 被动调 Q 的固态激光器具有体积小、成本低等优点,可用于紧凑型高重复频率脉冲激光器。特别在级联拉曼激光设计中,被动调 Q 压缩谐振腔,有利于增加腔内功率密度,提升拉曼转换,从而实现级联拉曼转换,获得普通固体激光难以实现的 1178 nm 和 1212 nm 等新波长的斯托克斯激光。相关波长倍频橙黄光在在钠导星、激光雷达和激光医疗等领域有重要应用[22−23],特别 1212 nm 对富含脂质组

收稿日期: 2023−02−21; **修订日期:** 2023−03−28

基金项目: 国家自然科学基金项目 (62275200); 温州市基础性科研项目 (G20220014); 浙江省新苗人才计划课题项目

作者简介: 齐子钦, 女, 本科生, 主要从事新型固体激光器方面的研究。

通讯作者: 朱海永, 男, 教授, 博士, 主要从事激光及非线性光学方面的研究。

织具有吸收亲和性，可用于刺激皮下组织脂肪细胞，是激光辅助皮肤愈合和预防疤痕形成的理想来源[24−25]。文中利用 Nd:YAG/Cr^{4+}:YAG 被动调 Q 激光驱动的 KTA 晶体，结合腔镜对腔内各阶斯托克斯波长激光损耗控制，成功实现了 671 cm^{-1} 和 234 cm^{-1} 频移级联的 1 178 nm 和 1 212 nm 双波长激光输出。

1 实验装置设计

KTA 晶体拥有 234 cm^{-1} 和 671 cm^{-1} 两个较强的拉曼频移峰。由于其属于正交晶系的各向异性晶体，对不同拉曼构型对应频移的拉曼增益差异非常大[26]。文中采用如图 1 所示的激光系统，即利用 Nd:YAG/Cr^{4+}:YAG 被动调 Q 激光驱动 KTA 晶体。由于可饱和吸收晶体和激光晶体都是 YAG 基质，将可饱和吸收晶体 Cr^{4+}:YAG 与激光晶体 Nd:YAG 键合，可使系统更紧凑、更易于散热。激光晶体选用尺寸为 3 mm×3 mm×7 mm 的掺 Nd^{3+}浓度 1.0 at.% 的 Nd:YAG 晶体，可饱和吸收体选用尺寸为 3 mm×3 mm×3 mm 的 Cr^{4+}:YAG 晶体，初始透射率约为 85%。KTA 晶体沿 X 轴晶向切割，尺寸为 4 mm×4 mm×25 mm。被动调 Q 的 Nd:YAG 基频激光腔内是无偏振的，而无偏振激光沿 KTA 晶体 X 轴晶向激发拉曼光谱中 234 cm^{-1} 和 671 cm^{-1} 两个频移峰具有相当强度[21]，所以比较容易实现两个不同频移级联拉曼转换。

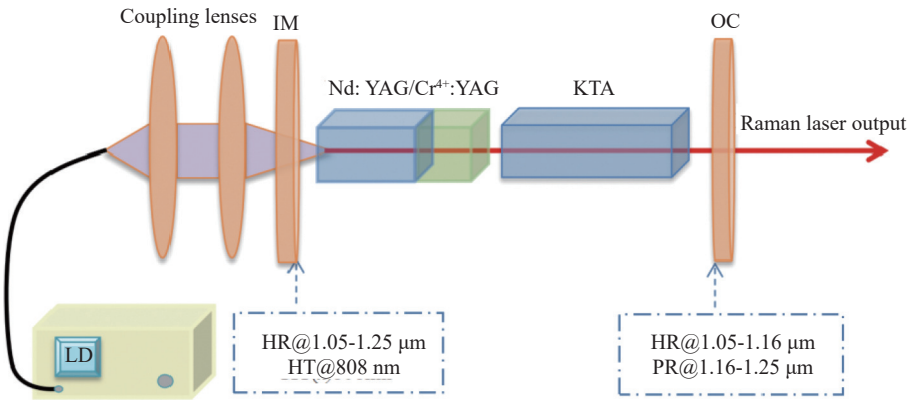

图 1 被动调 Q KTA 级联拉曼激光实验装置图

Fig.1 Experimental setup of passively Q-switched KTA cascade Raman laser

实验的抽运源采用中心波长为 808 nm 的光纤耦合输出的半导体激光器，其光纤芯径为 200 μm，数值孔径为 0.22。用一对消色差耦合透镜将抽运光聚焦到激光晶体内，该耦合系统聚焦后的束腰直径约为 320 μm。两块晶体用铟箔包裹放置在紫铜块中，通过半导体制冷模组 (TEC) 控温，使其温度均保持在 300 K 左右。由抽运输入镜 (IM) 和激光耦合输出镜 (OC) 组成的平凹腔保证了基频光和拉曼光有效振荡，腔内各光学元件紧凑布置，总腔长约为 50 mm。系统中，腔镜镀膜设计对级联拉曼实验至关重要。腔镜 IM 镀对 808 nm 抽运光高透 (T>95%)，并且对 1.05~1.25 μm 高反的膜系。腔镜 OC 为曲率半径为 500 mm 的平凹镜，并镀对 1.05~1.16 μm 波段高反，从 1.16~1.25 μm 波段部分透过率的膜系。具体的镀膜参数如图 2 所示，图中还给出了基于 234 cm^{-1} 和 671 cm^{-1} 频移的斯托克斯波长的透过率。基于实验谐振腔参数，可以计算得到当热透镜焦距为 25 cm 时，对应泵浦模式比 1∶1，晶体处的基模半径刚好为 160 μm；基模半径随透镜焦距减小而缩小。

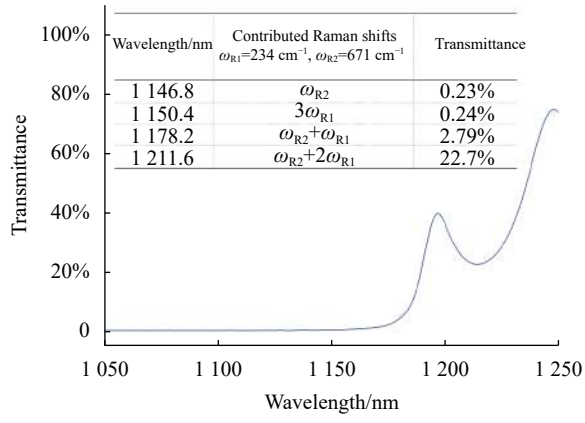

图 2 腔镜 OC 在不同斯托克斯波长的透过率

Fig.2 Transmittance of cavity mirror OC at different Stokes wavelengths

2 实验结果与分析

在激光调节过程中，随着激光输出功率变强，发现有几十毫瓦较强的黄光激光产生。用型号 AvaSpec-3648 光纤光谱仪测量了该黄光光谱，如图 3 所示，其中心波长位于 573.4 nm。为保证测量近红外波段拉曼激光功率的纯度，采用对可见光波段增透，对 1.05~1.25 μm 高反的分光镜将可见光分离测量。通过对激光系统的调节优化，实现了高效的级联拉曼激光输出。图 4 给出了用 Thorlabs 公司型号 PM310D 的功率计测量得到激光平均输出功率随入射抽运功率的变化值。图 5 给出了使用卓立汉光公司型号 Omni-λ500 光栅单色仪测量的不同功率下的激光波长。

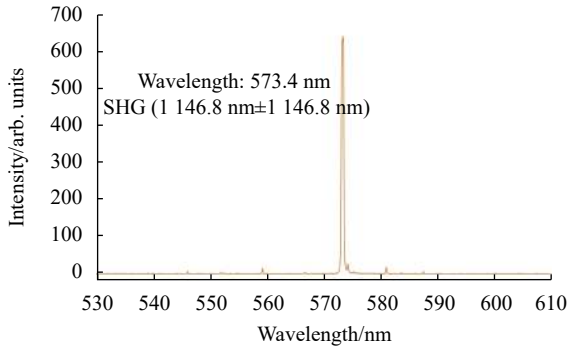

图 3 伴随拉曼激光输出的可见光光谱

Fig.3 Visible light spectra associated with Raman laser output

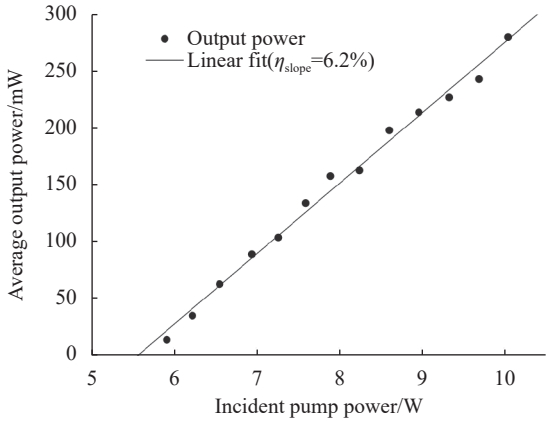

图 4 拉曼激光输出功率与入射抽运功率的关系图

Fig.4 Raman laser output power as a function of incident pump power

由图 4 可知 KTA 拉曼激光阈值约为 5.5 W，平均输出功率以 6.2% 斜率效率随着入射抽运功率增加而增加。在 10.05 W 的入射抽运功率下，获得了 280 mW 的平均输出功率，转化效率 2.8%。结合图 5 的激光波长可知，在阈值附近到 8 W 抽运功率下的输出激光波长以 1 178 nm 为主，同时伴随微弱的 1 146 nm 波长。其中 1 146 nm 激光是基频 1 064 nm 激光通过 KTA 晶体 671 cm^{-1} 频移获得的一阶斯托克斯激光，而 1 178 nm 激光是分别经过 234 cm^{-1} 和 671 cm^{-1} 频移各一次得到的斯托克斯激光。随着抽运功率的进一步提升，出现了 1 212 nm 波长激光。该波长激光为经过 671 cm^{-1} 一次频移和 234 cm^{-1} 两次频移级联的斯托克斯激光。随着入射抽运功率的逐渐增强，1 212 nm 这条谱线在总输出强度所占的比重也有所增大。在 10.05 W 的抽运下，获得了 1 178 nm 和 1 212 nm 同时输出的双波长激光。从最高抽运功率下的激光光谱图还可以看到非常弱的 1 182 nm 的激光谱线，该谱线为 1 064 nm 基频激光经过四次 234 cm^{-1} 频移得到四阶斯托克斯波长。由于腔镜在 1.05~1.16 nm 的高反射，抑制了 234 cm^{-1} 频移的一~三阶斯托克斯激光输出，到四阶斯托克斯波长的光强已较弱。其中 234 cm^{-1} 频移的一阶和二阶斯托克斯激光还是会经过 671 cm^{-1} 频移获得 1 178 nm 和 1 212 nm 的激光，但 234 cm^{-1} 频移的三阶和四阶斯托克斯激光以及 1 146 nm 倍频的黄绿激光产生会对 1 178 nm 和 1 212 nm 的激光产生增益竞争，一定程度上影响了最终的激光效率。

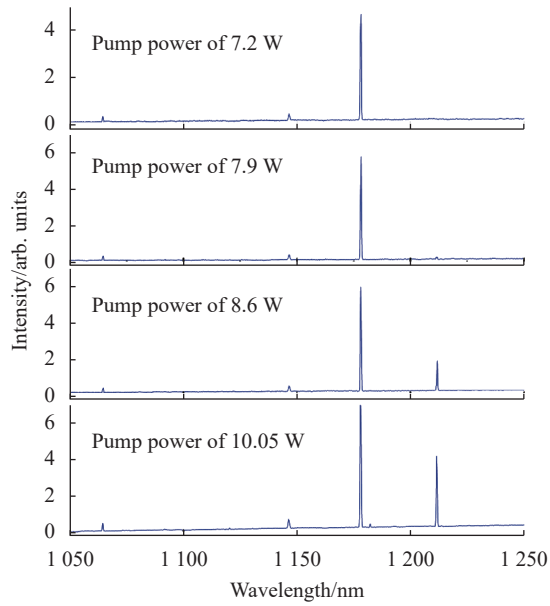

图 5 不同入射抽运功率下 KTA 级联拉曼的输出激光光谱

Fig.5 Output laser spectra of KTA cascade Raman at different incident pump powers

进一步采用型号 DET08 C/M 的 InGaAs 光电探测器 (带宽 5 GHz, 上升沿 70 ps) 和示波器对被动调 Q 的激光脉冲进行测量。结果表明脉冲重复频率随着入射抽运功率的增加而增加，而脉冲宽度在 1.5~1.1 ns 范围波动。图 6 给出了脉冲重复频率和计算得到的单脉冲能量随着抽运功率的变换关系图。脉冲重复频率在 5.9 W 抽运功率下为 1.9 kHz 上升到 10.05 W 抽运功率下为 10.3 kHz。单脉冲能量随着抽运功率快速增加，然后趋于稳定，这符合被动调 Q 的脉冲特性。根据被动调 Q 脉冲形成机理可知，随着功率的提高，可饱和吸收体会更快地被“漂白”，从而使形成脉冲的周期变短，重复频率快速增加，而保持单脉冲能量相对稳定。最高抽运功率下实测脉冲序列和单脉冲波形如图 7 所示。脉冲序列较为稳定，重复频率为 10.3 kHz，脉冲宽度在 1.2 ns 左右。

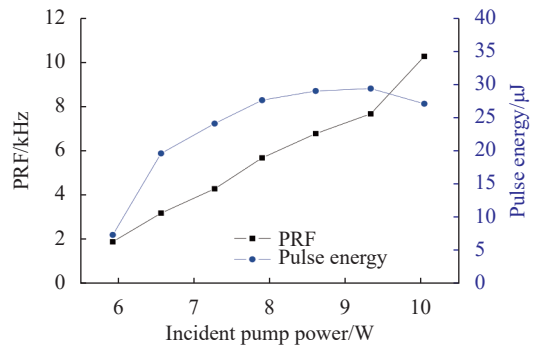

图 6 输出重复频率和脉冲能量与入射抽运功率的关系曲线

Fig.6 Pulse repetition frequency and pulse energy as a function of incident pump power

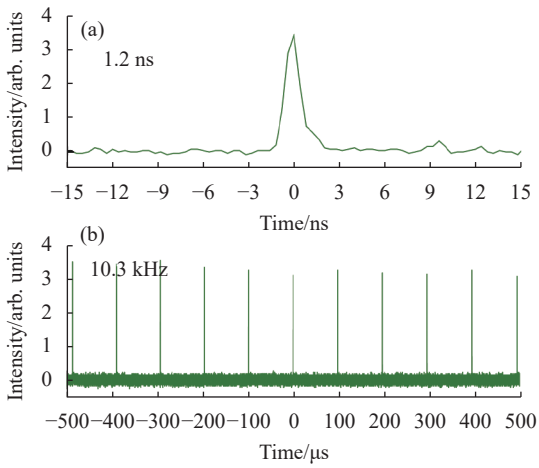

图 7 在 10.05 W 的入射抽运功率下测得的脉冲波形和序列

Fig.7 Temporal pulse profile and pulse train of the yellow laser emission as measured under an incident pump power of 10.05 W

3 结 论

文中对端面抽运 Nd:YAG/Cr^{4+}:YAG 被动调 Q 激光驱动的 KTA 晶体级联拉曼激光进行实验，研究了不同入射抽运功率下级联拉曼激光的输出功率、光谱和脉冲特性。通过选择腔镜控制腔内各阶斯托克斯波长的激光损耗，成功实现了 671 cm^{-1} 和 234 cm^{-1} 频移级联的 1.2 μm 波段斯托克斯激光输出。随着抽运功率的增加，输出激光波长从以 671 cm^{-1} 和 234 cm^{-1} 频移级联拉曼的 1 178 nm 单波长过渡到与 1 212 nm 同时输出的双波长。实验中也发现了高阶斯托克斯光和拉曼自倍频对腔内激光增益的竞争。最终入射泵抽运功率为 10.05 W 时，测得的最大平均输出功率为 280 mW。测量的脉冲宽度约为 1.2 ns，脉冲重复频率约为 10.3 kHz。对应单脉冲能量和峰值功率分别为 27.2 μJ 和 22.7 kW。考虑 1 178 nm 和 1 212 nm 波长的特殊应用，进一步实验可通过严格控制两个波长的损耗，实现单波长的激光输出。因此，基于 KTA 两个相当增益强度的频移，结合腔镜镀膜控制可以获得丰富 KTA 晶体高阶斯托克斯激光波长拓展固体激光应用。

参考文献：

[1] Pack M V, Armstrong D J, Smith A V. Measurement of the $\chi^{(2)}$ tensors of $KTiOPO_4$, $KTiOAsO_4$, $RbTiOPO_4$, and $RbTiOAsO_4$ crystals [J]. ***Applied Optics***, 2004, 43(16): 3319-3323.

[2] Gao Z L, Sun Y X, Yin X, et al. Growth and electric-elastic properties of $KTiOAsO_4$ single crystal [J]. ***Journal of Applied Physics***, 2010, 108(2): 024103.

[3] Bai Fen, Wang Qingpu, Liu Zhaojun, et al. Comparison of signal-resonant and idler-resonant KTA-SROs [J]. ***Chinese Optics Letters***, 2016, 14(7): 071402.

[4] Duan Y M, Zhu H Y, Xu C W, et al. Compact self-cascaded KTA-OPO for 2.6 μm laser generation [J]. ***Optics Express***, 2016, 24(23): 26529-26535.

[5] Bian Jintian, Kong Hui, Xu Haiping, et al. Temperature tuning properties of 3.5-μm $KTiOAsO_4$ optical parametric oscillator [J]. ***Chinese Journal of Lasers***, 2021, 48(4): 0401015. (in Chinese)

[6] Meng Jun, Li Chen, Cong Zhenhua, et al. Investigations on beam quality improvement of an NCPM-KTA-based high energy optical parametric oscillator using an unstable resonator with a Gaussian reflectivity mirror [Invited] [J]. ***Chinese Optics Letters***, 2022, 20(9): 091401.

[7] Watson G H. Polarized Raman spectra of $KTiOAsO_4$ and

isomorphic nonlinear-optical crystals [J]. ***Journal of Raman Spectroscopy***, 1991, 22(11): 705-713.

[8] Zhu H Y, Shao Z H, Wang H Y, et al. Multi-order Stokes output based on intra-cavity $KTiOAsO_4$ Raman crystal [J]. ***Optics Express***, 2014, 22(16): 19662-19667.

[9] Huang Y J, Chen Y F, Chen W D, et al. Dual-wavelength eye-safe Nd: YAP Raman laser [J]. ***Optics Letters***, 2015, 40(15): 3560-3563.

[10] Zhang Ximei, Chen Simeng, Shi Shencheng, et al. Study on the performance of cascaded Nd: $GdVO_4$ self-Raman laser at 1 309 nm [J]. ***Infrared and Laser Engineering***, 2019, 48(11): 1105002. (in Chinese)

[11] Sun Bing, Ding Xin, Jiang Pengbo, et al. Efficient wavelength-locked 878.6 nm diode-modulated-pumped Nd: YVO_4 self-Raman laser [J]. ***Infrared and Laser Engineering***, 2021, 50(12): 20200227. (in Chinese)

[12] Duan Y M, Sun Y L, Zhu H Y, et al. YVO_4 cascaded Raman laser for five-visible-wavelength switchable emission [J]. ***Optics Letters***, 2020, 45(9): 2564-2567.

[13] Bai Zhenxu, Chen Hui, Zhang Zhanpeng, et al. Hundred-watt dual-wavelength diamond Raman laser at 1.2/1.5 μm (Invited) [J]. ***Infrared and Laser Engineering***, 2021, 50(12): 20210685. (in Chinese)

[14] Yang Ce, Chen Meng, Ma Ning, et al. Picosecond multi-pulse burst pump KGW infrared multi-wavelength Raman laser [J]. ***Infrared and Laser Engineering***, 2020, 49(11): 20200044.

[15] Liu Z J, Wang Q P, Zhang X Y, et al. Coexistent optical parametric oscillation and stimulated Raman scattering in $KTiOAsO_4$ [J]. ***Optics Express***, 2008, 16(21): 17092-17097.

[16] Zhu H Y, Guo J H, Duan Y M, et al. Efficient 1.7 μm light source based on KTA-OPO derived by Nd: YVO_4 self-Raman laser [J]. ***Optics Letters***, 2018, 43(2): 345-348.

[17] Huang H T, Wang H, Wang S Q, et al. Designable cascaded nonlinear optical frequency conversion integrating multiple nonlinear interactions in two $KTiOAsO_4$ crystals [J]. ***Optics Express***, 2018, 26(2): 642-650.

[18] Liu Z J, Wang Q P, Zhang X Y, et al. 1120 nm second-Stokes generation in $KTiOAsO_4$ [J]. ***Laser Physics Letters***, 2008, 6(2): 121-124.

[19] Lan W X, Wang Q P, Liu Z J, et al. A diode end-pumped passively Q-switched Nd: YAG/KTA Raman laser [J]. ***Optik***, 2013, 124(24): 6866-6868.

[20] Duan Y M, Zhu H Y, Wang H Y, et al. Comparison of 1.15 μm Nd: YAG\KTA Raman lasers with 234 and 671 cm^{-1} shifts [J]. ***Optics Express***, 2016, 24(5): 5565-5571.

[21] Mao W J, Zhang D, Lu H Q, et al. Compact passively Q-switched KTA self-frequency doubled Raman laser with 671 cm^{-1} shift [J]. ***Optics and Laser Technology***, 2022, 156: 108619.

[22] Sheng Q, Lee A, Spence D, et al. Wavelength tuning and power enhancement of an intracavity Nd: $GdVO_4$-$BaWO_4$ Raman laser using an etalon [J]. ***Optics Express***, 2018, 26(24): 32145-32155.

[23] Sheng Q, Li R, Lee A, et al. A single-frequency intracavity Raman laser [J]. ***Optics Express***, 2019, 27(6): 8540-8553.

[24] Centurion P, Noriega A. Fat preserving by laser 1210-nm [J]. ***Journal of Cosmetic and Laser Therapy***, 2013, 15(1): 2-12.

[25] Philandrianos C, Bertrand B, Andrac-Meyer L, et al. Treatment of keloid scars with a 1210-nm diode laser in an animal model [J]. ***Lasers in Surgery and Medicine***, 2015, 47: 798-806.

[26] Liu Z J, Wang Q P, Zhang, X Y, et al. Self-frequency-doubled $KTiOAsO_4$ Raman laser emitting at 573 nm [J]. ***Optics Letters***, 2009, 34(14): 2183-2185.

End-pumped Nd:YAG/Cr^{4+}:YAG/KTA passive Q-switched cascade Raman laser

Qi Ziqin[1], Mao Wenjie[1], Wang Hongyan[2], Zhu Xiaolong[1], Qiu Xinnan[1], Lu Huanqia[1], Zhu Haiyong[1*]

(1. Wenzhou Key Laboratory of Micro-Nano Optoelectronic Devices, College of Electrical and Electronic Engineering, Wenzhou University, Wenzhou 325035, China;
2. Crystech Inc., Qingdao 266100, China)

Abstract:

Objective KTA crystal as Raman gain medium has attracted increasing attention. Its larger Raman gain and smaller Raman shift make it more advantageous for cascade Raman conversion to obtain new wavelength Stokes laser of 1 178 nm and 1 212 nm. The frequency doubling of both two Stokes laser could realize yellow and orange

emissions which have important applications in remote sensing, laser medicine and so on. In particular, 1 212 nm laser has an absorption affinity for lipid-rich tissues and can be used to stimulate adipose cells and mesymal fine tissue in subcutaneous tissues, which is an ideal source for laser assisted skin healing and prevention of excessive scar formation. In view of the important applications of 1 178 nm and 1 212 nm laser, KTA cascade Raman operation driven by passive Q-switched laser for these two wavelengths generation was further investigated.

Methods The laser system for KTA cascade Raman operation is shown (Fig.1). Nd:YAG/Cr^{4+}:YAG composite was used for passive Q-switched laser generation. Cr^{4+}:YAG crystal, with an initial transmittance of about 85%, was used as saturable absorber crystal and diffusion bonded to Nd:YAG crystal to make the laser system more compact and easy to dissipate heat. An *x*-axis cut KTA crystal with 25 mm in length was used as the Raman crystal. The plano-concave cavity with the total cavity length of about 50 mm guarantees the effective oscillation of the fundamental laser and Raman laser. The specific coating parameters are shown (Fig.2). The transmittance of Stokes wavelengths based on the Raman shift of 234 cm^{-1} and 671 cm^{-1} is also given (Fig.2).

Results and Discussions With the increase of Raman laser output power, we found the Stokes laser was accompanied by a small amount of yellow laser output, and the corresponding yellow light spectrum was shown (Fig.3). Under an incident pumping power of 10.05 W, an average output power of 280 mW was obtained, and the conversion efficiency is 2.8%. The output power and laser wavelength are shown (Fig.4-5). From the threshold to 8 W incident pump power, the main intensity laser wavelength was 1 178 nm, accompanied by a weak 1 146 nm wavelength. With the further increase of incident pump power, 1 212 nm wavelength laser appeared. As the incident pump power gradually further increased, the proportion of 1 212 nm line in the total output intensity also increased. A dual-wavelength laser with 1 178 nm and 1 212 nm output was obtained under the incident pump power of 10.05 W. The results show that the third- and fourth- Stokes laser generation with a Raman shift of 234 cm^{-1}, as well as the yellow laser produced by frequency doubling of 1 146 nm would lead to gain competition, and reduce the conversion efficiency of Stokes laser at 1 178 nm and 1 212 nm. The recorded pulse profile and pulse train at the highest output power are shown (Fig.7). The pulse repetition frequency was 10.3 kHz and the pulse width was about 1.2 ns. The compact passive Q-switched Raman laser cavity increased the power density, and resulted in the improvement of the Raman conversion, so as to realize the high-order Stokes waves.

Conclusions In this study, a diode end-pumped passive Q-switched cascade Raman laser with the Raman shifts of 671 cm^{-1} and 234 cm^{-1} based on KTA crystal is reported. Nd:YAG/Cr^{4+}:YAG composite crystal is used to generate pulsed fundamental laser and then to drive KTA crystal. The output power, spectrum and pulse characteristics of cascade Raman laser with different incident pump power are studied. With the increasing pump power, the output laser wavelength shifted from single wavelength of 1 178 nm based on 671 cm^{-1} and 234 cm^{-1} cascaded Raman shifts to dual-wavelength output of 1 178 nm and 1 212 nm. Under an incident pump power of 10.05 W, a dual-wavelength laser with an average output power of 280 mW and a conversion efficiency of 6.2% was obtained. The corresponding pulse width and pulse repetition frequency are 1.2 ns and 10.3 kHz, respectively. The single pulse energy and peak power are 27.2 μJ and 22.7 kW, respectively. The results show that rich Stokes laser wavelengths could be obtained based on two comparable gain Raman shifts of KTA crystal with the coating control of the cavity mirror.

Key words: Raman laser; KTA crystal; passive Q-switch; YAG crystal

Funding projects: National Natural Science Foundation of China (62275200); Basic Scientific Research Project of Wenzhou City (G20220014); Research Funds of College Student Innovation of Zhejiang Province